Biomaterials 32 (2011) 4021–4029

Contents lists available at ScienceDirect

Biomaterials

journal homepage: www.elsevier.com/locate/biomaterials

Tumor-homing photosensitizer-conjugated glycol chitosan nanoparticles for synchronous photodynamic imaging and therapy based on cellular on/off system

So Jin Lee [a,b,1], Heebeom Koo [a,1], Dong-Eun Lee [a], Solki Min [a,c], Seulki Lee [d], Xiaoyuan Chen [d], Yongseok Choi [b], James F. Leary [e], Kinam Park [e], Seo Young Jeong [c], Ick Chan Kwon [a], Kwangmeyung Kim [a,*], Kuiwon Choi [a,*]

[a] Biomedical Research Center, Korea Institute of Science and Technology, 39-1 Hawolgok-dong, Seongbuk-gu, Seoul 136-791, South Korea
[b] School of Life Science and Biotechnology, Korea University, 1 Anam-dong, Seongbuk-gu, Seoul 136-701, South Korea
[c] Department of Life and Nanopharmaceutical Science, Kyung Hee University, 1 Hoegi-dong, Dongdaemun-gu, Seoul 130-701, South Korea
[d] Laboratory of Molecular Imaging and Nanomedicine, National Institute of Biomedical Imaging and Bioengineering (NIBIB), National Institutes of Health (NIH), 31 Center Drive, Suite 1C14, Bethesda, MD 20892-2281, United States
[e] Departments of Biomedical Engineering and Pharmaceutics, Purdue University, West Lafayette, IN 47907, United States

ARTICLE INFO

Article history:
Received 17 December 2010
Accepted 4 February 2011
Available online 3 March 2011

Keywords:
Photosensitizer
Nanoparticle
Photodynamic therapy
Drug delivery
Glycol chitosan
Cellular on-off system

ABSTRACT

Herein, we developed the photosensitizer, protoporphyrin IX (PpIX), conjugated glycol chitosan (GC) nanoparticles (PpIX–GC–NPs) as tumor-homing drug carriers with cellular on/off system for photodynamic imaging and therapy, simultaneously. In order to prepare PpIX–GC–NPs, hydrophobic PpIXs were chemically conjugated to GC polymer and the amphiphilic PpIX–GC conjugates formed a stable nanoparticle structure in aqueous condition, wherein conjugated PpIX molecules formed hydrophobic inner-cores and they were covered by the hydrophilic GC polymer shell. Based on the nanoparticle structure, PpIX–GC–NPs showed the self-quenching effect that is 'off' state with no fluorescence signal and phototoxicity with light exposure. It is due to the compact crystallized PpIX molecules in the nanoparticles as confirmed by dynamic light scattering and X-ray diffraction methods. However, after cellular uptake, compact nanoparticle structure gradually decreased to generate strong fluorescence signal and singlet oxygen generation when irradiated. Importantly, PpIX–GC–NPs-treated mice presented prolonged blood circulation, enhanced tumor targeting ability, and improved *in vivo* therapeutic efficiency in tumor-bearing mice, compared to that of free PpIX-treated mice. These results proved that this tumor-homing cellular 'on/off' nanoparticle system of PpIX–GC–NPs has a great potential for synchronous photodynamic imaging and therapy in cancer treatment.

1. Introduction

Photodynamic therapy (PDT) is becoming widely known for its application in cancer therapy [1–4]. PDT is a medical treatment using chemical photosensitizer and light irradiation at certain wavelength onto target tumor tissues [5]. The light irradiation causes the photosensitizer to generate cytotoxic singlet oxygen that destroys tumor cells through apoptosis or necrosis [6]. In addition, the selective accumulation of photosensitizers like protoporphyrin IX (PpIX) in tumor tissues provides an intense fluorescence signal that also can be employed in photodynamic imaging (PDI) [7]. However, these photosensitizers are limited in clinical use because of non-specific skin phototoxicity, poor water solubility, and inefficient delivery to target tumor tissues in cancer treatment [8,9].

There are two strategies used for overcoming these limitations. The one is to enhance the tumor specificity of photosensitizer by using nano-sized drug carriers that are known to accumulate at the tumor site by the so-called enhanced permeation and retention (EPR) effect, resulting in efficient passive accumulation in solid tumor tissues [10]. It has been reported that various photosensitizer-encapsulated nano-sized carriers could enhance the tumor target specificity and therapeutic efficacy in cancer treatment, compared to free photosensitizer [2,3,11]. On the other hand, there are some efforts to control the photosensitizer's activity using quenching/dequenching system, which show the specific recovery of the photosensitizer's activity in target tumor tissue [7]. For this purpose, the quenched nano-sized drug carriers have been

* Corresponding authors. Tel.: +82 2 958 5916; fax: +82 2 958 5909.
E-mail addresses: kim@kist.re.kr (K. Kim), choi@kist.re.kr (K. Choi).
[1] These authors contributed equally to this paper.

0142-9612/$ – see front matter © 2011 Elsevier Ltd. All rights reserved.
doi:10.1016/j.biomaterials.2011.02.009

developed to recover the quenched photosensitizer's activity under tumor-specific stimuli such as tumoral acidic pH or tumor-specific enzymes [12,13], whereas the carriers at normal state presented the 'off' state with no fluorescence signal and phototoxicity with light exposure, due to the quenching effect. These quenching/dequenching system which 'turn on' at the target sites, such as target cell interior or tumor site, have provided the higher specificity over the photosensitized production of $^1O_2$ in cancer treatment. Unfortunately, *in vivo* studies have shown that the tumor targeting and specificity of various nano-sized drug carrier was not as high as anticipated. This is because that their tumor targeting ability and specificity have not been as good as one would expect, due to the *in vivo* instability, immunogenicity, and non-specific targeting in normal tissues, etc. [14,15].

Previously we also developed PpIX-loaded glycol chitosan (GC) nanoparticles that showed the higher tumor specificity in tumor-bearing mice [3]. However, the instability of physically loaded PpIX molecules in the nanoparticles might cause the burst drug release profile during the circulation *in vivo*. This undesirable disadvantage of PpIX-loaded nanoparticles caused the lower tumor target specificity and the unintended damage to normal tissues [15]. Herein, we rationally designed the PpIX-conjugated GC nanoparticles (PpIX–GC–NPs) based on cellular 'on/off' system for synchronous PDI and PDT in cancer treatment. In order to produce PpIX–GC–NPs, the hydrophobic sensitizers, PpIXs, were directly conjugated to GC polymer, and they can self-assemble to form stable nanoparticles in aqueous condition. The quenching/dequenching system of PpIX–GC–NPs were carefully assayed without or with sodium dodecyl sulfate (SDS), confirmed by measuring the changes in particle size and crystalline structure [16,17]. Also, the particle-structure switchable 'on' system of PpIX–GC–NPs in the production of single oxygen generation was examined in the cell culture system. Finally, the tumor targeting specificity and anti-cancer therapeutic efficacy of PpIX–CG–NPs were evaluated with HT-29 cancer xenograft model.

2. Materials and methods

2.1. Materials

Glycol chitosan (M_w = 250 kDa; degree of deacetylation = 82.7%), protoporphyrin IX (PpIX), N-hydroxysuccinimide (NHS), and 1-ethyl-3-(3-dimethylaminopropyl)-carbodiimide hydrochloride (EDC), dimethyl sulfoxide (DMSO), methylthiazolyldiphenyl-tetrazolium bromide (MTT), and sodium dodecyl sulfate (SDS) were purchased from Sigma (St. Louis, MO). 9,10-anthracenedipropionic acid (ADPA) purchased from Invitrogen (Carlsbad, CA, USA). All other chemicals and solvents were analytical grade and used without further purification.

2.2. Preparation of PpIX–GC–NPs

In order to prepare PpIX-conjugated glycol chitosan nanoparticles (PpIX–GC–NPs), first, hydrophobic PpIX was chemically conjugated to GC polymer. Glycol chitosan (100 mg, 0.4 μmol) was dissolved in a distilled water (10 ml) and PpIX (12.4 mg, 22 μmol) were dissolved in DMSO (2 ml), followed by the addition of 30 μmol of NHS and 30 μmol of EDC into DMSO solution. After the complete dissolution, each sample was mixed slowly and gently stirred. After 1day, the reaction mixture was dialyzed for 3 days against methanol/water mixed solution to remove free PpIX molecules by using a dialysis tube (Molecular cutoff = 12–14 kDa, Spectrum®, Rancho Dominquez, CA). Finally, the product was filtered with a 0.8 μm syringe filter (Cellulose acetate, Millipore) and then freeze-dried to give a green powder, in resulting PpIX–GC conjugates. The degree of chemical conjugation of PpIX in the PpIX–GC conjugates was measured using a Lambda UV–vis 7 spectrophotometer (Perkin–Elmer, CT). The synthesized PpIX–GC conjugates were dissolved in 2 ml of DMSO to give a clear solution. The PpIX's concentration in the conjugates was quantified by measuring the PpIX's absorbance at 370 nm, based on the standard concentration curve of free PpIX in DMSO.

Second, PpIX–GC–NPs were prepared by a simple sonication and self-assembly as below. A suspension of PpIX–GC conjugates in distilled water was sonicated three times each for a total of 2 min-pulse period using a probe-type sonicator (Sigma High Intensity Ultrasonic Processor, GEX-600) at 90 W in 6 s-intervals (5 s-pulse application; 1 s-off) to minimize the increase in temperature. After sonification, the solution was filtered with a 0.8 μm syringe filter and then used *in vitro* and *in vivo* studied. The recovery yield of nanoparticles after filtration was about >90% according to the weight measurement, and size distribution was hardly changed after filtration.

2.3. Particle analysis of PpIX–GC–NPs

The average size of PpIX–GC–NPs in aqueous condition was observed by using dynamic light scattering (DLS, 127-35 laser, spectra physics, Mountain View, CA). The size distribution of PpIX–GC–NPs (1 mg/ml in PBS) was also measured using BI-9000AT digital autocorrelator (Brookhaven, NY, USA), operated at 633 nm and 37 °C. The spherical morphology of PpIX–GC–NPs was observed using transmission electron microscopy (TEM, CM30 electron microscope, Philips, CA), that was operated at an acceleration voltage of 80 kV. The PpIX–GC–NP solution (1 mg/ml in distilled water) was placed on a 300-mesh copper grid coated with carbon, followed by drying the sample in room temperature. Negative staining was performed using a droplet of 2 wt% uranyl acetate solution. X-ray diffraction images were also achieved by same sample preparation procedure and TEM microscope.

2.4. Fluorescence quenching effect and singlet oxygen generation of PpIX–GC–NPs

In order to assay the quenching effect of PpIX–GC–NPs, the fluorescence intensity of PpIX–GC–NPs in distilled water or 5 wt% SDS solution was compared to that of free PpIX. After dissolving each sample (50 μg/ml) in 96 well plates, the fluorescence intensity of free PpIX and PpIX–GC–NPs was determined using a 12-bit CCD camera (Image Station 4000 MM; Kodak, New Haven, CT) equipped with a special C-mount lens and a long wave emission filter (600–700 nm; Omega Optical). Also, the quantitative fluorescence intensity of each sample was measured using fluorometer (ISS, Champaign, IL).

The generation of singlet oxygen was observed chemically using a singlet oxygen sensor, disodium salt of 9,10-anthracenedipropionic acid (ADPA), that is bleached by singlet oxygen to the corresponding endoperoxide [18]. To measure the singlet oxygen generation, 1 ml of free PpIX (10 μM) or PpIX–GC–NP (10 μM of PpIX) in D_2O or 5 wt% SDS solution was added into 150 μl of the 5.5 mM of ADPA solution in quartz cubette. After mixing each solution, it was completely bubbled with water-saturated oxygen for 10 min and irradiated with a 633 He–Ne laser. The optical density at 400 nm (λ_{max} of ADPA) was monitored every 2 min in a spectrophotometer (ISS, Champaign, IL).

2.5. In vitro cellular uptake and phototoxicity of PpIX–GC–NPs in the cell culture system

SCC-7 cells (squamous cell carcinoma, ATCC, Rockville, MD) are cultured in RPMI 1640 containing 10% FBS. SCC-7 Cells (1×10^5) were seeded onto 6-well plate and grown for 2 days. In order to tracking the polymer carrier, GC polymers of PpIX–GC–NPs (10 mg) were labeled with 0.1 wt% of FITC in 1 ml of DMSO [3]. RPMI 1640 containing 5 μg of FITC-labeled GC–PpIX was added, and the cells were incubated for 5, 10, 30 min, 1 h at 37 °C. And then, the cells were washed with PBS and fixed for 5 min with 4% paraformaldehyde. The subcellular localization and dequenching effect of PpIX–GC–NPs were imaged by Zeiss LSM 510 Meta NLD confocal microscope (Carl Zeiss Inc., Germany). Each fluorescence image was observed with FITC filter set (Ex = 488 nm, Em = band pass 500–550 nm) for FITC-labeled glycol chitosan polymer and TRITC filter set (Ex = 633 nm, Em = band pass 676–719 nm) for PpIX [3].

In order to assay the phototoxicity of PpIX–GC–NPs in the cell culture system, SCC-7 cells (1×10^4) were seeded onto 96 well plate and incubated with free PpIX, GC, and PpIX–GC–NPs (5 μg/ml of free PpIX) for 1 h. After the incubation, all cells were illuminated with a He–Ne laser (633 nm, 3 mW/cm^2) for pre-determined irradiation time. After 12 h post-incubation in dark condition, the phototoxicity of each sample was evaluated cell viability and apoptosis using MTT (Sigma, St. Louis, MO), and TUNEL assay was also performed with 12 min-irradiated samples using commercial cell death detection kit (TAKARA Bio Inc).

2.6. In vivo imaging of PpIX–GC–NPs in tumor-bearing mice

Athymic nude mice (5 weeks old, Institute of Medical Science, Tokyo) were used for animal experiments. Subcutaneous tumors were established by inoculating HT-29 cells (1.0×10^6) onto the backs of mice. When tumors grew to approximately 150–200 mm^3 in volume, free PpIX and PpIX–GC–NPs containing 20 mg/kg of free PpIX were intravenously injected via the tail vein into the tumor-bearing mice. After i.v. injection, the tumor tissues were imaged by positioning mice on an animal plate heated to 37 °C in the eXplore Optix System (Advanced Research Technologies Inc., Montreal, Canada). A 670 nm pulsed laser diode was used to excite PpIX molecules and the emitted long wave fluorescence (600–700 nm) was detected with a fast photomultiplier tube (Hamamatsu, Japan) and a time-correlated single photon counting system (Becker and Hickl GmbH, Berlin, Germany). To compare the biodistribution of free PpIX and PpIX–GC–NPs in normal tissues (liver, lung, spleen, kidney, and heart) and tumor tissue, after 3 day post-injection, the mice were sacrificed and each tissue was excised. The fluorescence intensity of PpIX in each

tissue was measured using a 12-bit CCD camera (Image Station 4000 MM; Kodak, New Haven, CT) with a special C-mount lens and a long wave emission filter (600–700 nm; Omega Optical). The fluorescence intensity in each tissue was recorded as total photons per centimeter squared per steradian ($p/s/cm^2/sr$) per each organ ($n = 3$ mice per group).

2.7. In vivo photodynamic therapy

To compare therapeutic efficacy of free PpIX and PpIX–GC–NPs, subcutaneous HT-29 tumor model were established onto the backs of mice in similar methods with imaging experiments (Section 2.6.). When the tumors grew to about 50 mm^3 in volume ($n = 5$), saline, free PpIX (20 mg/kg) and PpIX–GC–NPs (20 mg/kg of free PpIX) were intravenously injected via a tail vein. After 1 day post-injection, solid tumors were irradiated with a 633 nm laser (He–Ne laser, 3 mW/cm^2) for 30 min. Then, we monitored the therapeutic efficacy of saline, free PpIX, and GC–PpIX-treated mice and the tumor volumes were calculated as width × length × height × 1/2 with a caliper for 14 days [12]. Differences between experimental and control groups were determined using one-way ANOVA and deemed statistically significant (indicated by an asterisk (*) in figure) if $p < 0.01$.

3. Results and discussion

3.1. Synthesis and characterization of PpIX–GC–NPs

Herein, we designed the PpIX-conjugated GC nanoparticles (PpIX–GC–NPs) based on a cellular 'on/off' system for PDI and PDT in cancer treatment. As shown in Fig. 1a, to make PpIX-conjugated glycol chitosan nanoparticles (PpIX–GC–NPs), free PpIX molecules were directly conjugated the amine moieties of glycol chitosan polymer in the presence of NHS and EDC as coupling agents. After the reaction, we confirmed the formation of the amide linkage between glycol chitosan and PpIX by FT-IR (the amide peak at 1655 cm^{-1}). On average, PpIX–GC conjugates had the 42.4 ± 2.3 molecules of PpIX in the one glycol chitosan polymer, confirmed by a UV–vis spectrum. At this optimized reaction condition, PpIX–GC conjugates produced self-assembled nanoparticle structure with an average diameter of about 280 ± 3.5 nm as determined by DLS and its nano-sized spherical shape was also observed in TEM image (Fig. 1b and c). This nano-size of PpIX–GC–NPs was stably maintained at least after one week in PBS showing the good stability of GC–NPs in physiological condition (data not shown). The result indicates that PpIX–GC–NPs may self-assemble to form stable nanoparticles in aqueous condition, wherein hydrophilic GC is on the outside shell due to a hydrophilic interaction with water, and the water-insoluble PpIXs form dense cores by hydrophobic interactions via π–π stacking of the phenanthrene rings and hydrogen bonding [19].

Based on the nanoparticle structure, the PpIX–GC–NP may be used as cellular 'on/off' photodynamic system, because the highly dense PpIX cores are quenched 'off' state and may not generate sufficient fluorescence or singlet oxygen (Fig. 1d). It was suggested that photosensitizers in high density are quenched state with minimum fluorescence and phototoxicity in cancer treatment [7]. However, after cellular uptake, the dense PpIX cores gradually may decrease integrity in intracellular environment [16,17], which induces PpIX to the 'on' state and their activity can be recovered to generate strong fluorescence and singlet oxygen when irradiated.

3.2. Particle structure-dependant on/off system of PpIX–GC–NPs

We firstly tested whether PpIX–GC–NPs can produce the particle structure-dependant on/off system of singlet oxygen generation without or with SDS [16,17,20,21]. It has been reported that the integrity of self-assembled nanoparticles conjugated with hydrophobic moieties decreased by adding surfactant components, and this phenomenon similarly occurred by intracellular proteins in cell cytosol [16,17,22,23]. We assumed that the harsh intracellular condition is capable of disrupting condensed nanoparticle structure and exposing the inside hydrophobic molecules from nanoparticles [16,23,24]. As expected, the PpIX–GC–NPs incubated in 1–5 wt% SDS solution increased the particle's size from 350 ± 15 nm to 640 ± 32 nm, compared to PpIX–GC–NPs in distilled water (size: 280 nm), indicating that the surfactant, SDS, could disrupt the highly dense PpIX hydrophobic cores in the

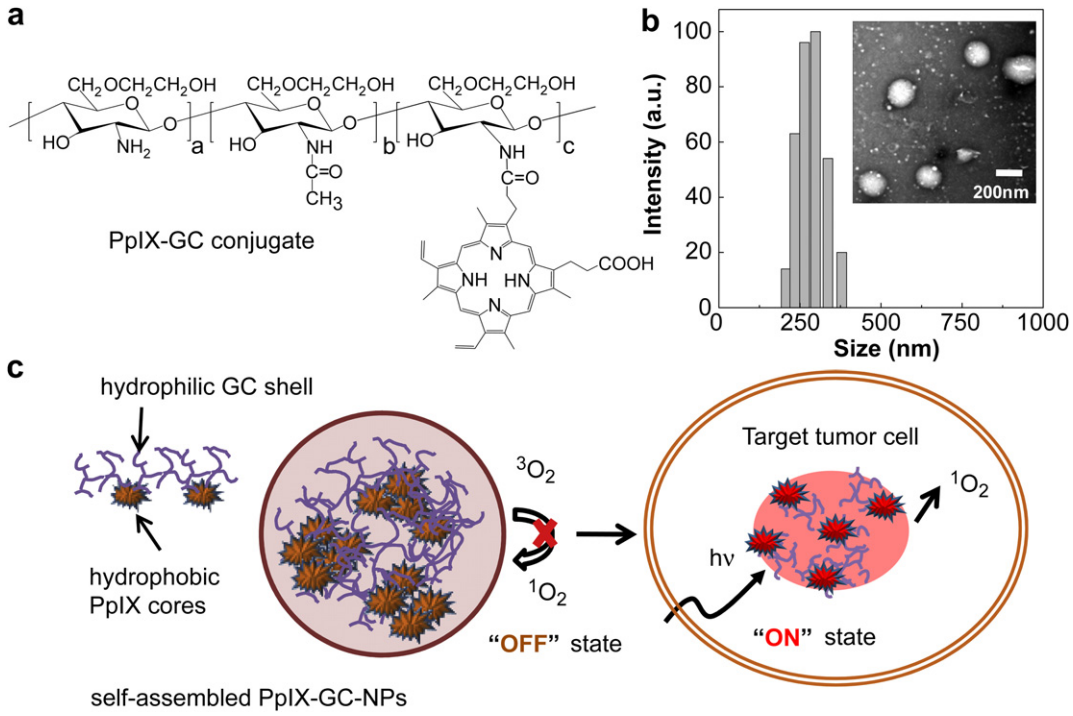

Fig. 1. Design and characterization of PpIX–GC–NP. (a) The chemical structure of PpIX–GC–NP. (b) Size and shape of PpIX–GC–NP determined by DLS and TEM image. (c) Scheme diagram of self-assembled PpIX–GC–NP and cellular 'on/off' system for synchronous photodynamic imaging and therapy of cancer.

nanoparticles [20] (Fig. 2a). It also suggests that the dense structure of the PpIX–GC–NPs may decrease the particle's integrity in cytosol mimic environment, which induce the quenched PpIX molecules to the 'on' state for singlet oxygen generation.

From the fluorescence imaging data, the fluorescence intensity of PpIX–GC–NPs in distilled water was completely quenched due to dense hydrophobic PpIX molecules in the nanoparticles even though under the higher PpIX's concentration of 50 μg/ml (Fig. 2b). When PpIX–GC–NPs were incubated in 5 wt% SDS solution for 1 h, the fluorescence intensity rapidly increased in proportion to the PpIX–GC–NPs concentration with light exposure. This result indicates that PpIX–GC–NPs substantially present the particle structure-dependant 'on/off' switching property in fluorescence imaging. As shown in Fig. 2c, the fluorescence intensity dramatically increased to 10-fold of that in distilled water. On the contrary, the fluorescence recovery of free PpIX was very smaller than that of

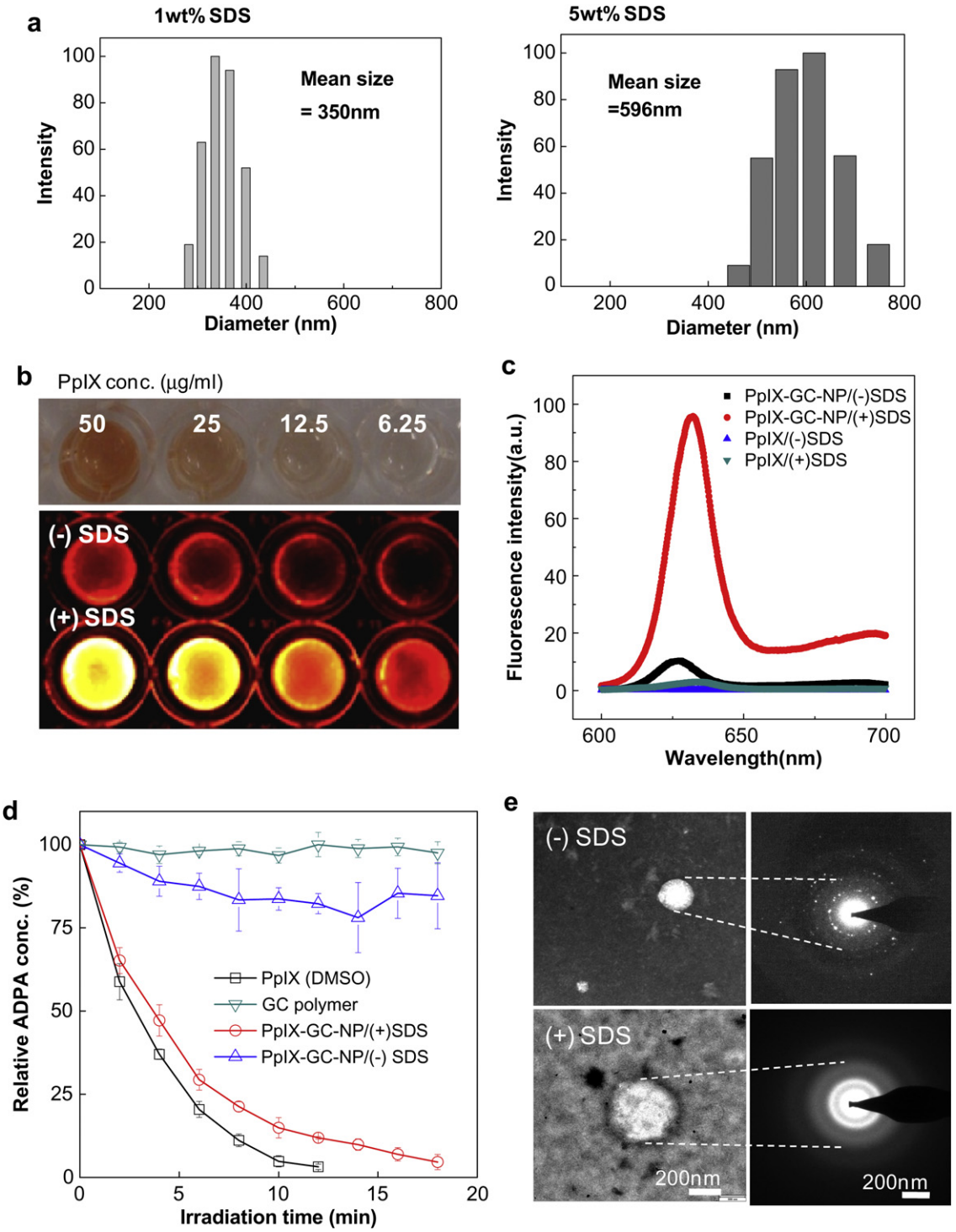

Fig. 2. Fluorescence and singlet oxygen generation of PpIX–GC–NP in cell free condition. (a) TEM images of PpIX–GC–NPs in 1% (left) and 5% (right) SDS aqueous solution. (b) Fluorescence imaging of 96-well microplates containing PpIX–GC–NP in water (upper) or 5% SDS aqueous solution (lower) (c) Fluorometer data of free PpIX and PpIX–GC–NP. (d) Singlet oxygen generation of GC–PpIX in water or 5 wt% SDS aqueous solution. (e) X-ray diffraction images of PpIX–GC–NP in water (upper) or 5 wt% SDS aqueous solution (lower).

PpIX–GC–NPs when the same concentration of SDS was treated. It means that the fluorescence on/off system of free PpIX molecules is not effective in the presence of SDS, compared to that of PpIX–GC–NPs.

To evaluate singlet oxygen generation characteristics of PpIX–GC–NPs without or with SDS, we measured the efficiency of $^1O_2$ generation using the disodium salt of 9,10-anthracenedipropionic acid (ADPA) as a singlet oxygen sensor (Fig. 2d). The control sample, pure GC polymer, and PpIX–GC–NPs in distilled water did not present any singlet oxygen generation, due to the strongly quenched state of PpIX molecules in the nanoparticles. However, PpIX–GC–NPs-treated with 5 wt% SDS showed a sharp decline in the presence of SDS, indicating rapid generation of $^1O_2$ with light exposure. It indicates that PpIX–GC–NPs can provide the particle structure-dependant specificity over the photosensitized production of $^1O_2$. We expect that PpIX–GC–NPs can produce specific phototoxicity in the target cancer cell environment, wherein the particles may lose their stable particle structure.

In addition, we further examined the precise structure of PpIX–GC–NPs via X-ray diffraction to confirm the crystalline structure of quenched PpIX molecules in the particles (Fig. 2e). In the distilled water, the 'off' state PpIX–GC–NPs showed a shining crystal structure with white spots due to the self-aggregated PpIX molecules in the nanoparticles [25]. This is deduced that $^1O_2$ sensitizers are very close enough to successfully quench each PpIX molecules in the nanoparticles with light exposure. As expected, however, the crystal structure of PpIX molecules rapidly disappeared in the presence of SDS, wherein PpIX molecules may present the 'on' system of florescence signal and singlet oxygen generation against laser irradiation. This X-ray diffraction data substantially presented the reasonable structural changes of PpIX molecules without or with surfactant molecules in aqueous condition. From the *in vitro* characterization data of PpIX–GC–NPs, we confirmed that PpIX–GC–NPs exhibited noticeable trends in recovery of fluorescence signal and singlet oxygen generation in the presence of SDS, demonstrating that PpIX–GC–NPs have the particle structure-dependant 'on/off' switching property for both PDI and PDT in cancer treatment.

3.3. Cellular uptake and in vitro phototoxicity of PpIX–GC–NPs in the cell culture system

Cellular uptake characteristic of PpIX–GC–NPs containing 5 μg/ml of free PpIX were evaluated using FITC-labeled PpIX–GC–NPs in the cell culture system. PpIX–GC–NPs showed fast cellular uptake within 10 min (Fig. 3a). After 10 min post-incubation, only green color of FITC-labeled GC polymer (FITC filter set: Ex = 488 nm, Em = 500–550 nm) was distributed throughout the cytoplasm, however, the PpIX molecules did not present any strong red fluorescence signal (TRITC filter set: Ex = 633 nm, Em = 676–719 nm), due to the self-quenching effect of PpIX molecules in the nanoparticles [19]. As time went on, red fluorescence intensity of PpIX molecules increased significantly in the cell, indicating that PpIX was restored to 'on' state with light exposure. This result is consistent with previous result of fluorescence recovery in the presence of surfactant, while PpIX was remained conjugated to GC polymers. As control, the fluorescence intensity of free PpIX molecules (5 μg/ml) was much lower than that of PpIX–GC–NPs. Previously, we reported that nanoparticle delivery system can increase their cell adhesion and cellular uptake of encapsulated or chemically conjugated PpIX molecules, compared to free PpIX molecules [3]. This high cellular uptake of PpIX–GC–NPs may be closely related to the enhanced phototoxicity in the cultured cell system, compared to that of free PpIX molecules.

Importantly, PpIX–GC–NPs reduced the phototoxicity of photosensitizer itself. Without light exposure, there was no significant cytotoxic effect in SCC-7 tumor cell culture system (Fig. 3b). However, free PpIX without irradiation treatment showed significant cytotoxicity for SCC-7 cells in dose-dependent manner, indicating that PpIX-conjugated nanoparticles may help to reduce the additional side effect of free photosensitizer *in vivo* [26]. As control, GC polymer showed a substantial biocompatibility in the cell culture system even at the higher concentration. After 1 h post-incubation, to evaluate the phototoxicity of PpIX–GC–NPs (5 μg/ml of PpIX), these cells were irradiated with a He–Ne laser (633 nm, 3 mW/cm^2) for 12 min. We observed that light-specific phototoxicity in the tumor cells induced by PpIX–GC–NPs using both MTT and TUNEL assay. After the light exposure, PpIX–GC–NPs-treated cells showed a substantial and proportional phototoxicity according to the irradiation time, due to the rapid production of singlet oxygen (Fig. 3c). Furthermore, PpIX–GC–NPs-treated cells presented an enhanced phototoxicity than free PpIX-treated cells, due to the particle's enhanced cellular uptake characteristics, as shown in Fig. 3a. Without light exposure, PpIX–GC–NP-treated cells did not present any apoptosis image after 6 h incubation. However, most PpIX–GC–NP-treated cells exhibited strong fluorescence signals indicative of apoptosis in TUNEL assay after 12 min irradiation following 6 h post-incubation. It really means that the harsh intracellular condition can be capable of particle structure-dependant 'on/off' system for singlet oxygen generation in cell culture system.

3.4. In vivo photodynamic imaging with PpIX–GC–NPs

By using the non-invasive optical imaging system, the tumor targeting ability of PpIX–GC–NPs was evaluated and compared to that of free PpIX and PpIX-loaded glycol chitosan nanoparticles (PpIX–CNPs) *in vivo* with HT-29 human colon adenocarcinoma tumor-bearing mice. As positive control, PpIX–CNPs were prepared by physical loading of free PpIX into hydrophobic 5β-cholanic acid modified glycol chitosan nanoparticles, as previously reported [3]. When the tumor size grew to about 150–200 mm^3, free PpIX, PpIX–CNPs and PpIX–NPs were intravenously injected via tail vein into tumor-bearing mice, wherein the PpIX concentration is 20 mg/kg in all samples. Fluorescence intensity and total photon count in the tumor region for each PpIX molecules in all samples was directly measured by imaging the fluorescence emission of PpIX itself (Fig. 4a). PpIX–GC–NP-treated mice exhibited the enhanced fluorescence intensity than that of free PpIX and PpIX–CNP in the tumor area at 1 h post-injection. The fluorescence signal of PpIX–GC–NP-treated mice gradually increased to 1 day and persisted for 3 days, indicating prolonged circulation, substantial tumor accumulation, and successful recovery of fluorescence intensity after cellular uptake of PpIX–GC–NPs, whereas in the case of free PpIX a relative weak fluorescence signal was detected at all time points. Within 1 day post-injection, PpIX–CNPs-treated mice as positive control, wherein PpIX molecules are physically loaded into the glycol chitosan nanoparticles, showed the similar tumor targeting specificity that of PpIX–GC–NPs. However, after 1 day post-injection, fluorescent signals in tumor tissue substantially decreased like free PpIX-treated mice, due to the rapid excretion of physically loaded free PpIX molecules from the tumor tissue. Particularly, PpIX–GC–NP-treated mice maintained the highest tumor target specificity up to 3 days, indicating that the chemically conjugated PpIX molecules successfully localized in tumor tissue. We also assayed the biodistribution of PpIX–GC–NPs in dissected tumors and other major organs (liver, lung, spleen, kidney, and heart). *Ex vivo* fluorescence images at 3 days after PpIX–GC–NP injection showed the highest fluorescence signal in tumor tissue but weak signals in other organs, indicating efficient accumulation in tumor

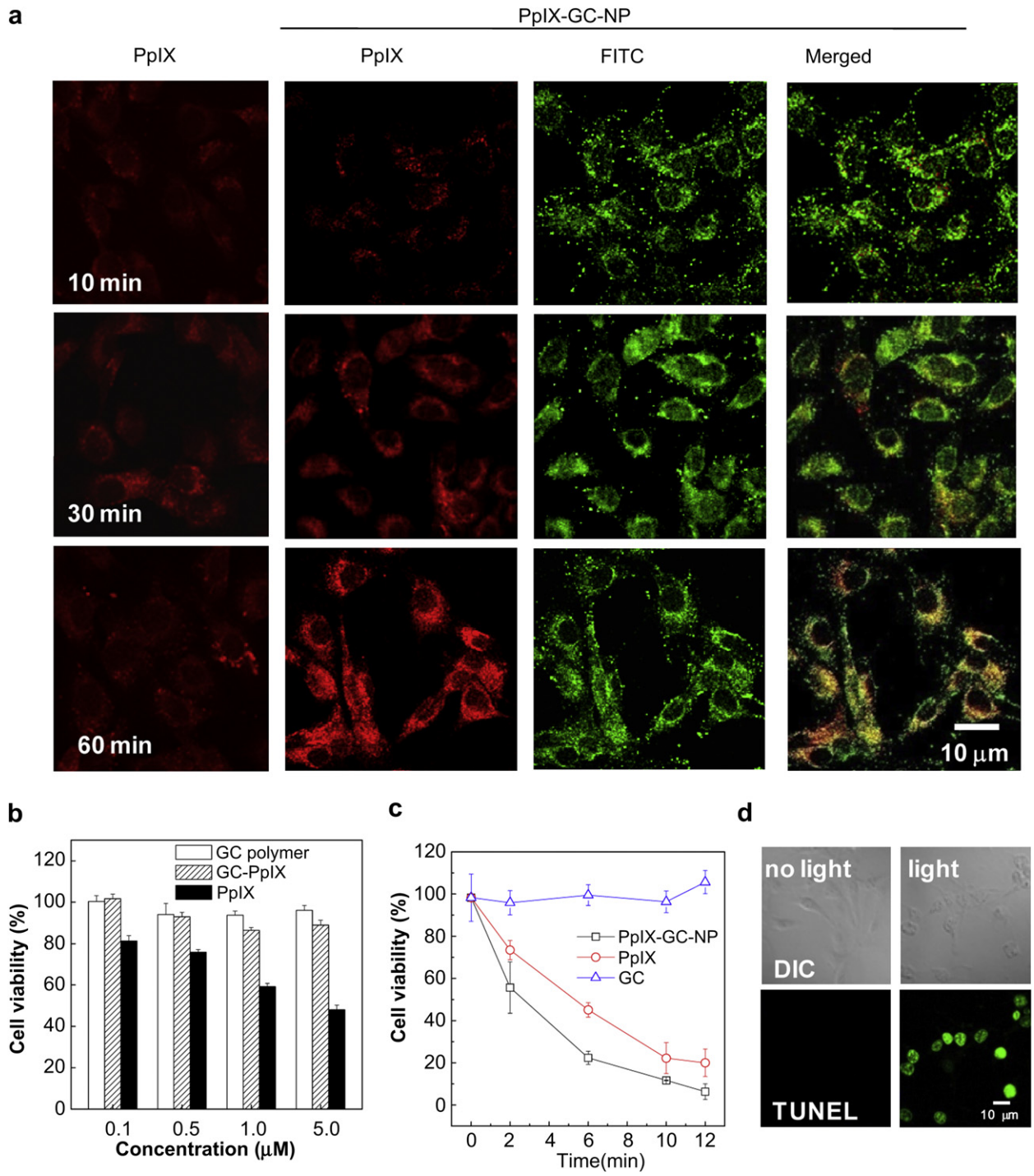

Fig. 3. *In vitro* fluorescence recovery of PpIX–GC–NP and photodynamic therapy. (A) Cellular uptake and time-dependent fluorescence recovery of PpIX–GC–NP in SCC-7 cells. (B) MTT assay against SCC-7 cells with different concentrations of free PpIX and PpIX–GC–NP after 1 h incubation in dark condition. (C) MTT assay against SCC-7 cells with free PpIX and PpIX–GC–NP according to laser irradiation time. (D) TUNEL stain images of SCC-7 cells incubated with PpIX–GC–NP before and after laser irradiation.

tissue, whereas the majority of free PpIX was uptake in the liver due to its high hydrophobicity (Fig. 4b). The total photon counts of PpIX–GC–NPs in tumor tissue are 1.41–2.1 folds higher than that of PpIX–CNP and free PpIX-treated mice, respectively (Fig. 4c). These results indicate that the conjugation of PpIX to GC polymer may help to increase retention of PpIX in tumor tissues for slow excretion from cells [27]. This selective delivery and accumulation of PpIX–GC–NPs in tumor region provides an intense fluorescence image that allows successive cancer-related diagnosis by PDI.

3.5. In vivo photodynamic therapy with PpIX–GC–NPs in tumor-bearing mice

When the tumor size grew to about 50 mm^3, we administered Free PpIX and PpIX–GC–NP (20 mg/kg of PpIX) into the tail vein of HT-29 tumor-bearing mice. At 12 h and 24 h after injection, all mice were irradiated with a He–Ne laser (633 nm, 3 mW/cm^2) for 30 min. After 1 day, PpIX–GC–NP-treated mice showed a clear hemorrhagic injury at the irradiation site, and severe cell death

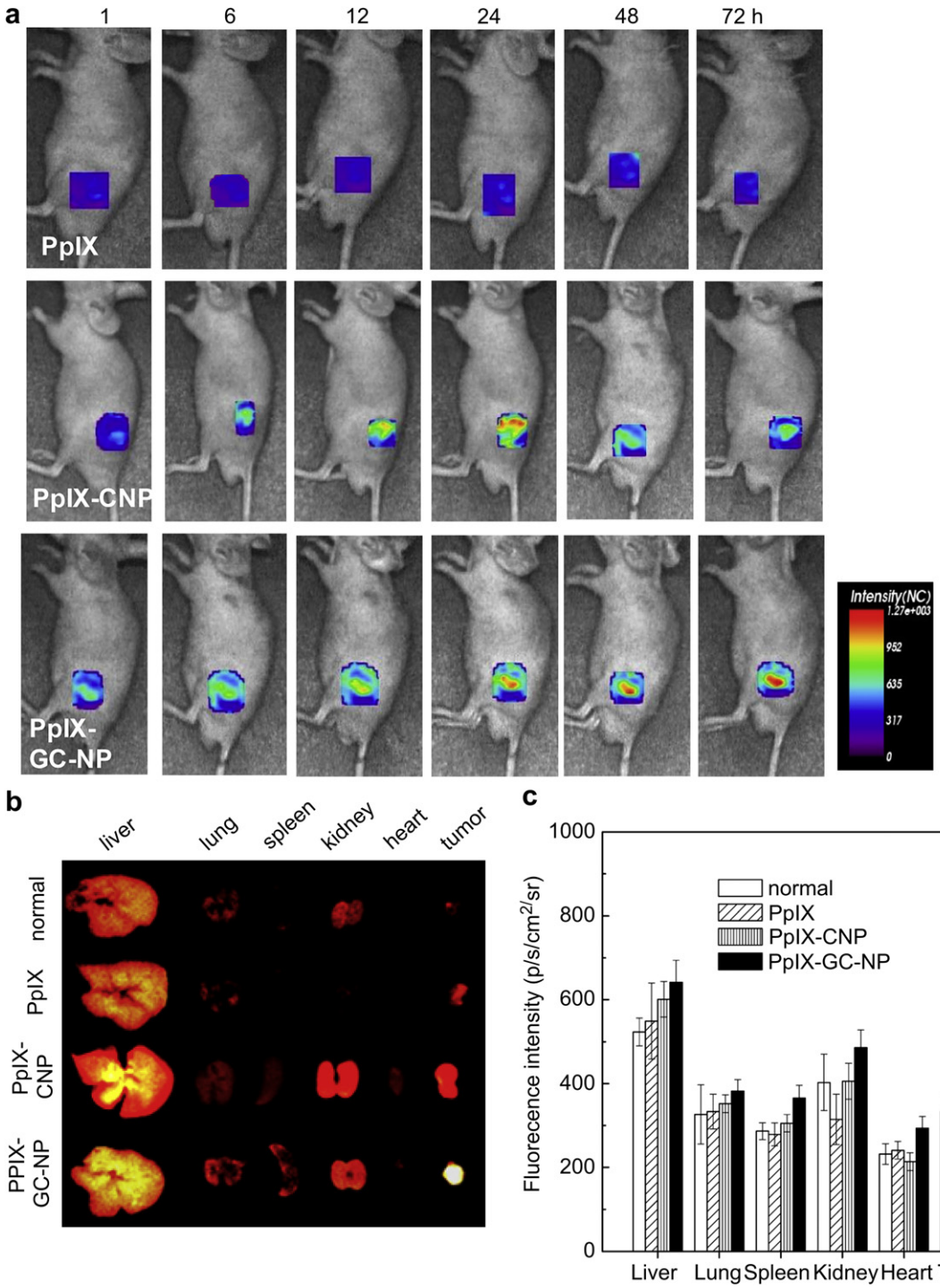

Fig. 4. *In vivo* tumor accumulation of PpIX–GC–NP and photodynamic imaging. (A) *In vivo* non-invasive fluorescence imaging of the PpIX–GC–NP accumulation at tumor site in HT-29 tumor-bearing mice. (B) *Ex vivo* images of major organs (liver, lung, spleen, kidney, and heart) and tumors excised at 3 days post-injeciton of saline, free PpIX and PpIX–GC–NP. (C) Total photon counts per centimeter squared per steradian (p/s/cm^2/sr) per each excised organ of free PpIX and PpIX–GC–NP was recorded as at 3 days post-injection in HT-29 tumor-bearing mice ($n = 3$).

occurred within 10 days (Fig. 5a). While free PpIX showed little therapeutic efficacy with only a small portion of the tumor showing cell death, and there was no severely damaged tissue. During 2 weeks, the tumor growth rate was compared in three groups of mice with saline, free PpIX, and PpIX–GC–NP (Fig. 5b). The size of tumors in mice with free PpIX was about 260 mm^3 after 14 days, and this value was not significantly different with the case of negative control, saline. This result may come from the poor production of singlet oxygen due to insufficient tumor accumulation of free PpIX. However, in the case of PpIX–GC–NP-treated mice, the tumor growth was successfully suppressed below 50 mm^3, showing the effective therapeutic result. The histological tissue images also proved the significant therapeutic efficacy of PpIX–GC–NP than that of free PpIX (Fig. 5c). After 14 days, the mice

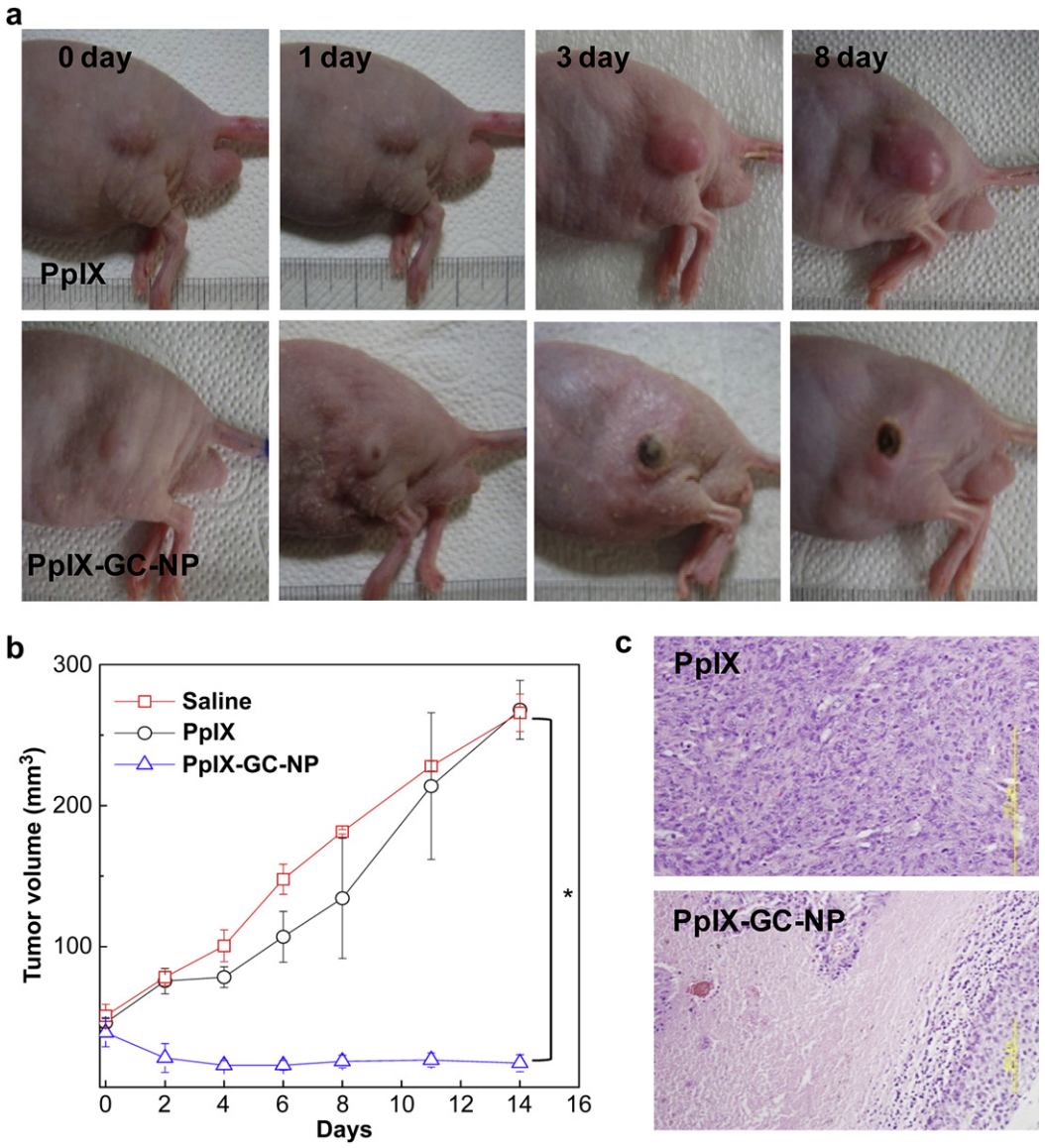

Fig. 5. *In vivo* photodynamic therapy with PpIX–GC–NP. (A) Tumor images of free PpIX and PpIX–GC–NP (20 mg/kg of PpIX) in photodynamic therapy. (B) Measured tumor growth for 14 days ($n = 5$). Data represent mean ± s.e. ($* = p < 0.01$ by one-way ANOVA).

were sacrificed, and each tumor tissue was obtained and H&E staining was performed. In case of free PpIX, only a small portion of apoptosis and necrosis were observed, confirming effective concentration of free PpIX was not delivered to tumors and the amount of generated singlet oxygen was insufficient. In contrast, PpIX–GC–NP-treated mice, large amount of cells in tumor tissue were severely dead, showing the successful results of PDT. Taken together, these results indicate that PpIX–GC–NPs efficiently localized to tumors and, following irradiation, produced cytotoxic singlet oxygen that induced tumor cell death and reduced tumor volume.

4. Conclusion

We synthesized PpIX–GC–NPs, the photosensetizer conjugated polymeric nanoparticle, and its cellular 'on/off' switching and *in vivo* tumor-homing ability was examined. In aqueous condition, PpIX–GC–NPs self-assembled to construct stable spherical structure with a mean diameter of about 280 nm. In the nanoparticles, PpIXs formed dense cores as a crystalline, and they were 'off' state via self-quenching with no fluorescence or singlet oxygen generation. However, after cellular uptake of their particles, intracellular severe environment decreased the integrity of dense structure and turned PpIX fluorescence 'on' and restored therapeutic activity. This cellular 'on/off' nanoparticle system can reduce unintended cytotoxicity and increase therapeutic efficacy after cellular uptake and irradiation. Furthermore, the PpIX–GC–NPs presented prolonged blood circulation, enhanced tumor-homing ability, and improved *in vivo* therapeutic efficiency in tumor-bearing mice. Therefore we can conclude that this tumor-homing cellular 'on/off' system, PpIX–GC–NP has great potential for synchronous PDI and PDT in cancer treatment.

Acknowledgements

This work was financially supported by the Real-Time Molecular Imaging Project, GRL Program of MEST, Fusion Technology Project (2009-0081876) of MEST, and by grant to the Intramural Research Program of KIST.

References

[1] Dolmans DEJGJ, Fukumura D, Jain RK. Photodynamic therapy for cancer. Nat Rev Cancer 2003;3:380–7.

[2] McCarthy JR, Perez JM, Brückner C, Weissleder R. Polymeric nanoparticle preparation that eradicates tumors. Nano Lett 2005;5:2552–6.

[3] Lee SJ, Park K, Oh Y, Kwon S, Her S, Kim I, et al. Tumor specificity and therapeutic efficacy of photosensitizer-encapsulated glycol chitosan-based nanoparticles in tumor-bearing mice. Biomaterials 2009;30:2929–39.

[4] Gao D, Xu H, Philbert Martin A, Kopelman R. Ultrafine hydrogel nanoparticles: synthetic approach and therapeutic application in living cells. Angew Chem Int Ed 2007;46:2224–7.

[5] Solban N, Rizvi I, Hasan T. Targeted photodynamic therapy. Lasers Surg Med 2006;38:522–31.

[6] Goswami LN, White WH, Spernyak JA, Ethirajan M, Chen Y, Missert JR, et al. Synthesis of tumor-avid photosensitizer–Gd(III)DTPA conjugates: impact of the number of gadolinium units in T1/T2 relaxivity, intracellular localization, and photosensitizing efficacy. Bioconjug Chem 2010;21:816–27.

[7] Lovell JF, Chen J, Jarvi MT, Cao W, Allen AD, Liu Y, et al. FRET quenching of photosensitizer singlet oxygen generation. J Phys Chem B 2009;113:3203–11.

[8] Sun Y, Chen Z, Yang X, Huang P, Zhou X, Du X. Magnetic chitosan nanoparticles as a drug delivery system for targeting photodynamic therapy. Nanotechnology 2009;20:135102.

[9] Guillemard V, Saragovi HU. Taxane-antibody conjugates afford potent cytotoxicity, enhanced solubility, and tumor target selectivity. Cancer Res 2001;61:694–9.

[10] Bechet D, Couleaud P, Frochot C, Viriot M, Guillemin F, Barberi-Heyob M. Nanoparticles as vehicles for delivery of photodynamic therapy agents. Trends Biotechnol 2008;26:612–21.

[11] Ideta R, Tasaka F, Jang W, Nishiyama N, Zhang G, Harada A, et al. Nanotechnology-based photodynamic therapy for neovascular disease using a supramolecular nanocarrier loaded with a dendritic photosensitizer. Nano Lett 2005;5:2426–31.

[12] Koo H, Lee H, Lee S, Min KH, Kim MS, Lee DS, et al. In vivo tumor diagnosis and photodynamic therapy via tumoral pH-responsive polymeric micelles. Chem Commun 2010;46:5668–70.

[13] Choi Y, Weissleder R, Tung C. Selective antitumor effect of novel protease-mediated photodynamic agent. Cancer Res 2006;66:7225–9.

[14] Simon V, Devaux C, Darmon A, Donnet T, Thiénot E, Germain M, et al. Pp IX silica nanoparticles demonstrate differential interactions with in vitro tumor cell lines and in vivo mouse models of human cancers. Photochem Photobiol 2010;86:213–22.

[15] Bae YH, Yin H. Stability issues of polymeric micelles. J Control Release 2008;131:2–4.

[16] Savić R, Azzam T, Eisenberg A, Maysinger D. Assessment of the integrity of poly(caprolactone)-b-poly(ethylene oxide) micelles under biological conditions: a fluorogenic-based approach. Langmuir 2006;22:3570–8.

[17] Chen H, Kim S, He W, Wang H, Low PS, Park K, et al. Fast release of lipophilic agents from circulating PEG-PDLLA micelles revealed by in vivo forster resonance energy transfer imaging. Langmuir 2008;24:5213–7.

[18] Zhang P, Steelant W, Kumar M, Scholfield M. Versatile photosensitizers for photodynamic therapy at infrared excitation. J Am Chem Soc 2007;129:4526–7.

[19] de Villiers KA, Marques HM, Egan TJ. The crystal structure of halofantrine-ferriprotoporphyrin IX and the mechanism of action of arylmethanol antimalarials. J Inorg Biochem 2008;102:1660–7.

[20] Vangeyte P, Leyh B, Auvray L, Grandjean J, Misselyn-Bauduin AM, Jérôme R. Mixed self-assembly of poly(ethylene oxide)-b-poly(ϵ-caprolactone) copolymers and sodium dodecyl sulfate in aqueous solution. Langmuir 2004;20:9019–28.

[21] Jansson J, Schillen K, Nilsson M, Soderman O, Fritz G, Bergmann A, et al. Small-angle X-ray scattering, light scattering, and NMR study of PEO–PPO–PEO triblock copolymer/cationic surfactant complexes in aqueous solution. J Phys Chem B 2005;109:7073–83.

[22] Allen TM, Cullis PR. Drug delivery systems: entering the mainstream. Science 2004;303:1818–22.

[23] Chen H, Kim S, Li L, Wang S, Park K, Cheng J-X. Release of hydrophobic molecules from polymer micelles into cell membranes revealed by Förster resonance energy transfer imaging. Proc Natl Acad Sci U S A 2008;105:6596–601.

[24] Kim CK, Ghosh P, Pagliuca C, Zhu Z, Menichetti S, Rotello VM. Entrapment of hydrophobic drugs in nanoparticle monolayers with efficient release into cancer cells. J Am Chem Soc 2009;131:1360–1.

[25] Bendersky LA, Gayle FW. Electron diffraction using transmission electron microscopy. J Res Natl Inst Stan 2001;106:997–1012.

[26] Chu E, Wu R, Yow C, Wong T, Chen J. The cytotoxic and genotoxic potential of 5-aminolevulinic acid on lymphocytes: a comet assay study. Cancer Chemother Pharmacol 2006;58:408–14.

[27] Bae B, Na K. Self-quenching polysaccharide-based nanogels of pullulan/folate-photosensitizer conjugates for photodynamic therapy. Biomaterials; 2010:6325–35 [31].